Science of the Total Environment 660 (2019) 1015–1028

Contents lists available at ScienceDirect

Science of the Total Environment

journal homepage: www.elsevier.com/locate/scitotenv

Changes in lateral floodplain connectivity accompanying stream channel evolution: Implications for sediment and nutrient budgets

William J. Beck [a,*], Peter L. Moore [a], Keith E. Schilling [b], Calvin F. Wolter [c], Thomas M. Isenhart [a], Kevin J. Cole [d], Mark D. Tomer [d]

[a] Iowa State University, Department of Natural Resource Ecology and Management, 2310 Pammel Dr., Ames, IA 50011, USA
[b] Iowa Geological Survey, University of Iowa, 340A Trowbridge Hall, Iowa City, IA 52242, USA
[c] Iowa Department of Natural Resources, Des Moines, IA 50309, USA
[d] United States Department of Agriculture Agricultural Research Service, National Laboratory for Agriculture and the Environment, 1015 N. University Blvd, Ames, IA 50011, USA

HIGHLIGHTS

- Channel-floodplain connectivity was quantified using field data and hydraulic modeling.
- Stream channel cross sectional area increased ~17% over a 16 year period.
- Fluxes of sediment and phosphorus to floodplain storage decreased with increased channel conveyance.
- Sediment and nutrient budgets should account for the impacts of channel evolution on floodplain storage.

GRAPHICAL ABSTRACT

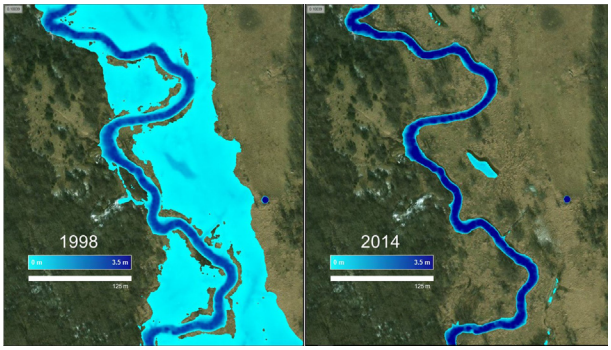

ARTICLE INFO

Article history:
Received 26 June 2018
Received in revised form 20 December 2018
Accepted 5 January 2019
Available online 7 January 2019

Keywords:
HEC-RAS
Channel geometry
Overbank flow
Floodplain storage
Phosphorus

ABSTRACT

Floodplain storage commonly represents one of the largest sediment fluxes within sediment budgets. In watersheds responding to large scale disturbance, floodplain-channel lateral connectivity may change over time with progression of channel evolution and associated changes in channel geometry. In this study we investigated the effects of channel geometry change on floodplain inundation frequency and flux of suspended sediment (SS) and total phosphorus (TP) to floodplain storage within the 52.2 km^2 Walnut Creek watershed (Iowa, USA) through a combination of 25 in-field channel cross section transects, hydraulic modeling (HEC-RAS), and stream gauging station-derived water quality and quantity data. Cross sectional area of the 25 in-field channel cross sections increased by a mean of 17% over the 16 year study period (1998–2014), and field data indicate a general trend of degradation and widening to be present along Walnut Creek's main stem. Estimated stream discharge required to generate lateral overbank flow increased 15%, and floodplain inundation volume decreased by 37% over study duration. Estimated annual fluxes of SS and TP to floodplain storage decreased by 61 and 62% over study duration, respectively. The estimated reductions in flux to floodplain storage have potential to increase watershed export of SS and TP by 9 and 18%, respectively. Increased contributions to SS and TP export may continue as channel evolution progresses and floodplain storage opportunities continue to decline. In addition to loss of storage, higher discharges confined to the channel may have greater stream power, resulting in further enhancement of SS and TP export through accelerated bed and bank erosion. These increased contributions to watershed loads may mask SS and TP reductions achieved through edge of field practices, thus making it critical that stage and

* Corresponding author.
E-mail addresses: wjbeck@iastate.edu (W.J. Beck), pmoore@iastate.edu (P.L. Moore), keith-schilling@uiowa.edu (K.E. Schilling), calvin.wolter@dnr.iowa.gov (C.F. Wolter), isenhart@iastate.edu (T.M. Isenhart), kevin.j.cole@ars.usda.gov (K.J. Cole), mark.tomer@ars.usda.gov (M.D. Tomer).

https://doi.org/10.1016/j.scitotenv.2019.01.038
0048-9697/

progression of channel evolution be taken into consideration when addressing sediment and phosphorus loading at the watershed scale.

1. Introduction

Lateral hydrologic connectivity between a stream channel and its floodplain (i.e., frequency and degree of floodplain inundation through lateral overbank flow) represents a vital pathway for the transfer and exchange of energy and materials between aquatic and terrestrial ecosystems (Junk et al., 1989; Tockner et al., 1999). This link has significant impacts on the life cycle and functioning condition of aquatic (Phelps et al., 2015) and terrestrial biota (Allen et al., 2016; Kaase and Kupfer, 2016; Batzer et al., 2018). Lateral connectivity provides a myriad of ecosystem services for society as well, notably the detention of flood waters (Tockner and Stanford, 2002), and the trapping and storage of sediment and nutrients delivered with inundating overbank flow (Venterink et al., 2003; Noe and Hupp, 2009; Hopkins et al., 2018).

Floodplain storage has been documented as a significant component of watershed sediment budgets (Walling et al., 1998), especially in systems experiencing aggradation in response to disturbance (Trimble, 1983). Floodplains have also been documented to store significant amounts of phosphorus (P) entering from inundating overbank flows (Kronvang et al., 2007), as P often moves in association with sediment. In addition to P, floodplains play an important role in the storage and cycling of nitrate within watersheds (Forshay and Stanley, 2005). Nitrate removal through denitrification within floodplain soils may be impacted by frequency and duration of floodplain inundation and spatial patterns of overbank sediment deposition (Orr et al., 2007; Pinay et al., 2000). Thus, the degree of lateral channel-floodplain connectivity may have important implications for sediment and nutrient budgets, as well as export, at the watershed scale.

A hydrologic separation between the channel and floodplain frequently occurs when changes in channel geometry increase channel conveyance. This change can occur naturally over millennia (e.g., following climatic shifts) or rapidly as a response to anthropogenic disturbance (e.g., channelization, landcover conversion). A significant body of work within unglaciated portions of southwest Wisconsin and northwest Illinois, USA, documented decreases in lateral channel-floodplain connectivity following landscape conversion-driven increases to channel cross sectional area (Knox, 2006, 1987, 1977; Lecce, 1997; Magilligan, 1985; Woltemade, 1994). In addition to reduced rates of floodplain sediment accretion, Knox (1987) reported the observed changes in channel morphology led to a near doubling of the discharge required to produce lateral overbank flow. Similar decreases in lateral connectivity following landcover conversion-driven changes to channel morphology were reported in the Georgia Piedmont, USA, as well (Ruhlman and Nutter, 1999). Despite the documented link between channel morphology and channel-floodplain lateral connectivity, consideration of morphological change is often absent from river basin management efforts, especially flood risk assessment (Lane et al., 2007; Raven et al., 2010; Sear et al., 1995).

In alluvial channels, response to disturbance may occur through a relatively consistent pattern of adjustments collectively known as the channel evolution model (CEM) (Schumm et al., 1984; Simon, 1989). These adjustments are frequently initiated by an increase in stream power and/or decrease in sediment supply relative to previous conditions. The initial response is for the channel to incise (referred to as stage III), followed by subsequent stages of degradation and widening (IV), and aggradation and widening (Stage V) before returning to relative stability (stage VI). It should be stated, however, that the CEM response is not universally applicable to all fluvial systems (Duvall, 2004; Stark, 2006), and that factors such as bed sediment dynamics and channel boundary conditions may influence a system's response to disturbance (Baker, 1977; Kondolf et al., 2002). Nevertheless, channel instability in alluvial systems and the CEM response hold global significance (Surian and Rinaldi, 2003; Wasson et al., 1998). Regionally, several studies from the U.S. Midwest (Schilling and Wolter, 2000; Palmer et al., 2014; Beck et al., 2018; Zaimes et al., 2004; Belmont et al., 2011; Midgley et al., 2012; Tufekcioglu et al., 2012; Willett et al., 2012) have documented unstable in-channel conditions (e.g., channel incision, streambank erosion) that suggest regional streams are experiencing adjustment-driven increases in cross sectional area.

If all else remains equal, the adjustment-driven increase in channel cross sectional area should lead to a corresponding increase in the maximum discharge that can be contained within the channel. We'll refer to this discharge as Q_t, as it is the threshold discharge above which portions of the floodplain may become inundated (i.e., bankfull discharge). A preliminary estimate of the magnitude of change in Q_t accompanying a change in channel cross sectional area may be outlined using a strategy similar to that of (Moody et al., 1999). Suppose that the depth d of an evolving channel changes by a factor of λ, (so that $d_2 = \lambda d_1$) and width w changes by a factor θ (so that $w_2 = \theta w_1$) between two observations, time 1 and time 2. According to Manning's equation ($Q = n^{-1} d^{5/3} w S^{1/2}$), the ratio of thresholds discharges between time 2 and time 1 is:

$$\frac{Q_{t2}}{Q_{t1}} = \left(\frac{\theta w_1}{w_1}\right)\left(\frac{\lambda d_1}{d_1}\right)^{5/3} = \theta\lambda^{5/3}, \quad (1)$$

assuming no change in channel roughness (n) or gradient (S). From this equation, a hypothetical 10% increase in channel depth ($\lambda = 1.1$) and a 10% increase in channel width ($\theta = 1.1$) would lead to a nearly 29% increase in threshold discharge ($1.1 \times 1.1^{5/3} = 1.289$). This estimate, however, assumes uniform and steady flow, which may be a poor approximation in real streams, particularly those that exhibit flashy hydrology. It nevertheless suggests that relatively small changes in channel cross-sectional area could have substantial effects on the discharge necessary to access the floodplain.

If floodplain inundation frequency and extent decrease as a channel enlarges as it progresses through stages III-V, a significant reduction in floodplain storage of suspended sediment (SS) and total phosphorus (TP) may occur. This reduction in floodplain storage is of importance, as it may lead to increases in watershed-scale SS and TP export. Thus, proper understanding and inclusion of geomorphological processes, such as changes in channel geometry, is critical when developing budgets and allocating sources and sinks of SS and TP at the watershed scale. Despite this, proper understanding and inclusion of geomorphological processes is frequently lacking in watershed-scale budgets (Reid and Dunne, 2003). In addition, studies that investigate floodplain inundation dynamics and flux of SS and TP to floodplain storage at the watershed scale are rare, due in part to the complexity of floodplain-channel interactions and computational effort required for modeling at that respective scale (Nicholas et al., 2006). Because of this, a great need exists for both practical, simplistic tools to investigate and quantify channel-floodplain lateral connectivity at the watershed scale (Newson and Large, 2006; Soar et al., 2017) and the utilization of these tools to address watershed scale sediment and TP dynamics.

For this study, we seek to estimate watershed-scale overbank flow dynamics and flux of SS and TP to floodplain storage in the context of channel evolution. We utilize a combination of in-field channel cross section measurements, hydraulic modeling, and stream gauging station-derived water quality and quantity data to investigate changes in floodplain inundation and storage over a 16 year period in Walnut Creek, Iowa, USA. We hypothesize that the increased channel cross

sectional area should increase the bankfull capacity of the channel. Without a corresponding increase in the duration of high-discharge events, this should reduce frequency of floodplain inundation and therefore reduce opportunities to store sediment and nutrients on the floodplain.

Our specific study objectives were to: 1) characterize channel geomorphic change along ~10 km of alluvial stream channel over a 16 year period; 2) estimate the effects of channel geomorphic change on overbank flow parameters and lateral channel-floodplain connectivity at the watershed scale; 3) estimate the effects of channel geomorphic change on flux of suspended sediment and total phosphorus to floodplain storage at the watershed scale, and 4) assess the implications of channel geomorphic change on watershed-scale SS and TP export.

2. Materials and methods

2.1. Study area

2.1.1. Watershed description

Walnut Creek is a perennial, third order stream draining 52.2 km^2 in Jasper County, Iowa, USA (Fig. 1). The Walnut Creek watershed is located in the Rolling Loess Prairies Level IV Ecoregion (47f), a region typified by rolling topography and well-developed drainage systems (Griffith et al., 1994). Walnut Creek is located within a humid, continental region with average annual precipitation of approximately 750 mm. The mean annual flood (2.33 year recurrence interval) from records at the watershed outlet gauging station is 30.5 m^3 s^{-1}, and the 5-year flood is approximately 37.1 m^3 s^{-1} based on 22 years of record (1995–2017). Watershed land use consists of 54% rowcrop agriculture (primarily corn-soybean rotation), 36% grassland, and 4% forest, with the remainder comprising roads, farmsteads, and urban areas (Schilling et al., 2006). Of the grassland area, 25.4% is recently restored tallgrass prairie established by the U.S. Fish and Wildlife Service (USFWS) as part of the Neal Smith National Wildlife Refuge (NSNWR). Since refuge creation in 1991, large tracts of row crop agricultural land have been converted to native tallgrass prairie.

Watershed soils are primarily silty clay loams, or clays formed in loess or till. The upland surficial geology is comprised of a 1–6 m loess cap overlaying pre-Illinoian glacial till, with Holocene alluvial deposits being comprised primarily of silty clay loams, clay loams, or silt loams (Schilling et al., 2009). A majority of watershed soils exhibit moderate to high erosion potential, with 54% being classified as highly erodible (Schilling and Thompson, 2000).

2.1.2. Channel and floodplain characteristics

The Walnut Creek channel is incised >3 m into its floodplain and is typified by tall, cohesive (i.e., >15% clay content) streambanks (Photo 1). The effects of historic agricultural-associated practices such as row crop conversion, stream straightening, subsurface drainage, and removal of riparian vegetation (Schilling and Wolter, 2000; Schilling et al., 2011), have led to a flashy hydrology, with Walnut Creek frequently exhibiting rapid responses to precipitation. Several stages of stream channel evolution have been documented through ~20 years of channel cross sectional measurements initiated by Schilling and Wolter (2000), with areas of Stage III (degradation), Stage IV (degradation and widening), and Stage V (aggradation and widening) present (Simon, 1989). Field observations indicate Stage IV as the most prevalent along Walnut Creek's main stem (Photo 2).

Walnut Creek's floodplain is comprised of a series of loess-derived Holocene alluvial deposits, collectively known as the DeForest Formation (Bettis, 1990). Three primary members of the DeForest Formation comprise the vertical profile of Walnut Creek's floodplain. The Gunder member occupies the lowest stratigraphic position at depths of 1–3 m (Schilling et al., 2009) and commonly comprises the streambank toe and streambed. The Gunder has been classified as a silt loam with massive structure, and exhibits a greater bulk density (1.6 g cm^{-3}) and sand content (28.5% by weight) relative to the other members (Beck et al., 2018). The Roberts Creek member (silty clay loam) overlies the Gunder,

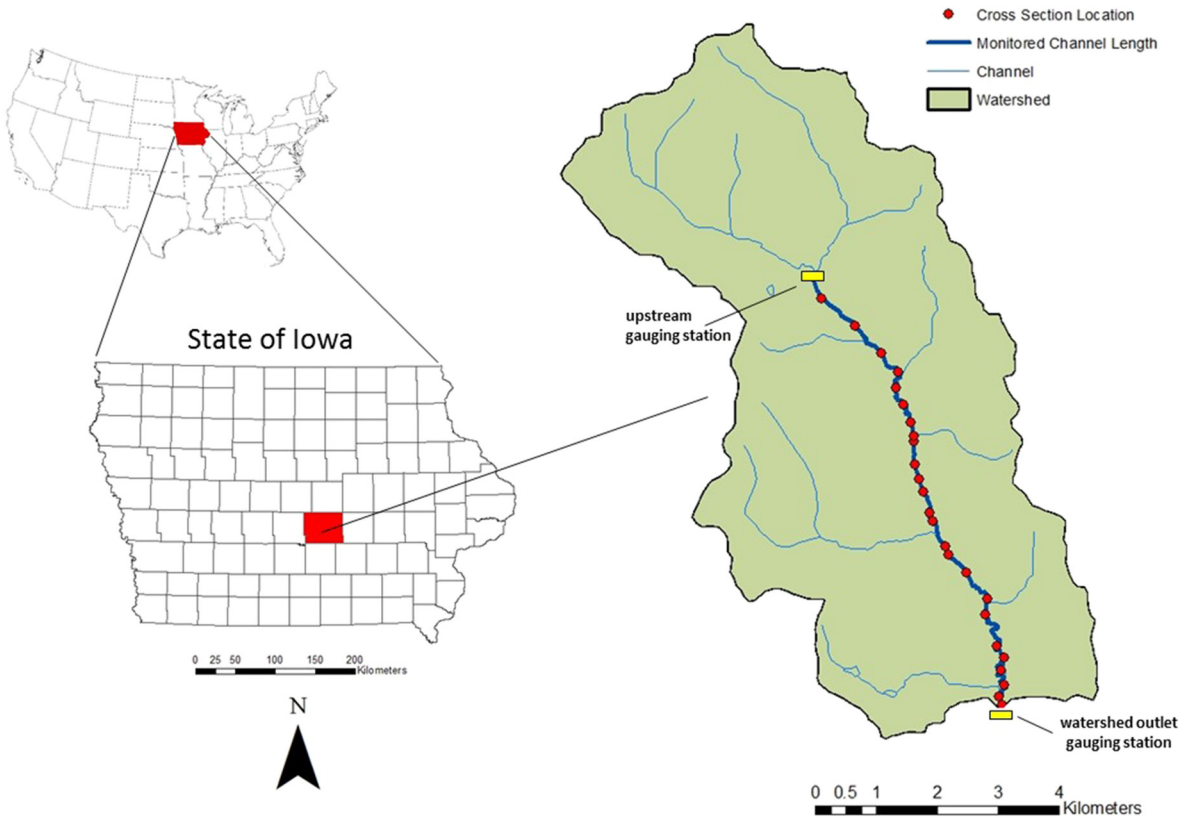

Fig. 1. Location of watershed, monitored channel length, and channel cross section transects, Walnut Creek, Iowa, USA.

Photo 1. Representation of the tall, cohesive streambanks and degree of channel incision present along the main stem of Walnut Creek, Iowa.

and represents the pre-European-American settlement landscape surface (Bettis et al., 1992). The Camp Creek member overlies the Roberts Creek and represents the upper stratigraphic position (i.e., floodplain surface). Camp Creek was deposited during the last ~400 years (Bettis et al., 1992), and is typically referred to as 'post-European-American settlement alluvium'. Camp Creek is described as a silt loam, and ranges in thickness from 0.6 to 1.8 m (Schilling et al., 2009). Distribution, stratigraphic position, thickness, and inherent soil characteristics (e.g., texture, bulk density) of the Camp Creek, Roberts Creek, and Gunder members have been documented as being consistent throughout the watershed (Schilling et al., 2009).

Monocultural expanses of reed canary grass (*Phalaris arundinacea*) dominate the current vegetative cover of Walnut Creek's floodplain. These expanses are frequently interspersed with low-density riparian forest, comprised primarily of Eastern Cottonwood (*Populus deltoides* Bartr.), Silver Maple (*Acer saccharinum* L.), Green Ash (*Fraxinus pennsylvanica* Marsh.), Black Walnut (*Juglans nigra* L.), Hackberry (*Celtis occidentalis* L.), White Mulberry (*Morus alba* L.), and Black Willow

Photo 2. Mass wasting of streambank material, indicative of Stage IV of stream channel evolution, Walnut Creek, Iowa.

(*Salix nigra* Marsh.). Along the outer floodplain fringe, landcover transitions to a mixture of row crop agriculture (i.e., corn-soybean rotation) and re-established native tallgrass prairie with increasing floodplain surface elevation.

2.2. Field measurements

During October 1998, researchers traversed ~10 km of Walnut Creek's main stem and established a series of 25 stream channel cross section transects (Schilling and Wolter, 2000) (Fig. 1). Transects were spaced every ~300 to 400 m, with locations selected to represent the range of channel form (e.g., meandering, straight) and condition (e.g., erosion activity, bed material) present in Walnut Creek. Cross sectional dimensions were measured by stretching a meter tape across the top of banks, perpendicular to the channel, and using a survey rod to record lateral distance along the tape and depth from the tape to the channel walls and streambed. Length-depth readings were recorded at each significant break in slope, as well as left and right edges of water and at the thalweg. End points for the cross-section locations were established using GPS-technology. During October 2014, transect locations were revisited and cross sectional dimensions measured using the identical rod-tape method.

2.3. Evaluation of channel-floodplain lateral connectivity

2.3.1. HEC-RAS models

Walnut Creek floodplain inundation frequency, discharge, and extent for the years 1998 and 2014 were quantified through creation of a pair of Hydrological Engineering Center River Analysis 5.0.1 (HEC-RAS) models (Brunner, 2016). HEC-RAS is a hydraulic model that uses the one-dimensional energy equation to calculate water surface elevations at a series of channel cross sections for given river discharge values. HEC-RAS was deemed an effective means of quantifying channel-floodplain connectivity as its outputs include floodplain inundation depth (m), velocity ($m\,s^{-1}$), and discharge ($m^3\,s^{-1}$) at individual channel cross sections, as well as cumulative floodplain inundation volume (m^3) and areal extent (m^2) for river reaches as a whole. The overbank flow duration outputs generated by HEC-RAS were used as a means to quantify change in floodplain SS and TP storage in light of the lack of widespread depositional field data available to researchers at time of study.

Individual HEC-RAS models were created for the years 1998 and 2014. Both models entailed merging respective field cross section transects with a 3 m digital elevation model (DEM) derived from 2010 aerial LiDAR. Lateral extents of field cross section transects were increased to span the entire left and right overbank floodplains. Models represented the entire ~10 km study length of Walnut Creek's main stem, which was divided into 7 individual reaches based on confluences with significant tributaries (Fig. 1). Reaches ranged in length from 264 to 2408 m. Inclusion of tributary flow allowed for 100% of watershed contributing area to be accounted for within the models. Manning's roughness coefficient (n) inputs for channel cross sections and floodplain areas were determined using an additive method outlined in Arcement and Schneider (1989). For both models, roughness coefficient (n) values ranged from 0.067 to 0.095 (floodplain) and from 0.041 to 0.064 (channel), with individual assignments based on in-field knowledge of floodplain and channel conditions (i.e., field notes, photographs). Model simulations were conducted under steady flow conditions (i.e., no change in discharge with time at individual cross sections) and subcritical (i.e., Froude number < 1.0) flow regimes.

HEC-RAS requires stream discharge inputs for each individual channel cross section. Discharge inputs for this study were derived from United States Geological Survey (USGS) and United States Department of Agriculture Agricultural Research Service (USDA-ARS) sub-hourly discharge data collected at the watershed outlet gauging station (Fig. 1). Sub-hourly discharge data were averaged to an hourly time series, and then used to create a flow duration curve (FDC) for the data availability period (1994–2017). FDCs display the percent of time that a particular stream discharge is exceeded over a given time period (Vogel and Fennessay, 1994). A mean hourly discharge time series was utilized to best capture rapid stormflow peaks characteristic of Walnut Creek's flashy hydrology. Mean hourly discharges were scaled from the watershed outlet gauging station to individual cross sections using discharge-drainage area relations (Biedenharn et al., 2000; Linhart et al., 2012). Discharge-drainage area estimates of cross-section discharge were validated using the FDC (1994–2017) of Walnut Creek's upstream gauging station.

2.3.2. Overbank threshold discharge

A range of higher-discharge (~10 to 71 $m^3\,s^{-1}$) stream flows were selected from the overall FDC and used as HEC-RAS inputs in an exploratory effort to identify overbank discharge thresholds for all individual cross sections in both models. The overbank threshold discharge for an individual channel cross section was defined as the discharge required to initially force streamflow to exit the channel and enter the floodplain on at least on side of the channel. Authors recognize that floodplain inundation could occur via saturation-overland flow from adjacent upland areas, however, for the purposes of this study we consider SS and TP flux to the floodplain to occur only when a direct hydraulic connection between channel and floodplain exists.

Threshold determination for each cross section was achieved through visual and numerical interpretation of HEC-RAS outputs. Visual determination was accomplished via RAS Mapper, a HEC-RAS feature which allows for aerial imagery to be overlain with simulated overbank flow extent. Numerically, overbank flow was determined to occur when discharge cross sectional area (m^2) exceeded that of channel cross sectional area (m^2). Threshold discharges were determined for both individual cross sections, as well as at the watershed-scale. Three watershed-scale thresholds were calculated for each model, and were represented by the watershed outlet mean hourly discharge: 1) stream discharge required to produce overbank flow at 100% of cross sections (hereafter referred to as *maximum discharge*), 2) stream discharge required to produce overbank flow at the majority (i.e., >50%) of cross sections (hereafter referred to as *majority discharge*), and 3) stream discharge at which only one cross section remains overbank (hereafter referred to as *minimum discharge*).

2.3.3. Floodplain storage

Floodplain storage quantification was initiated by selecting a range of watershed outlet FDC-derived discharge values as HEC-RAS inputs (Table 1). Selected discharges approximated the previously determined range of minimum to maximum overbank threshold discharges, and were thus deemed adequate to investigate change in overbank thresholds between years. In the HEC-RAS models, input discharge values were associated with a respective FDC-derived percent exceedance. Hereafter, these specific combinations of discharge and percent exceedance will be referred to as *discharge profiles*. HEC-RAS numerical outputs

Table 1
HEC-RAS discharge profiles used to quantify floodplain storage, Walnut Creek, Iowa. Data derived from watershed outlet gauging station FDC for years 1995–2017.

HEC-RAS discharge profile	Mean hourly discharge ($m^3\,s^{-1}$)	Exceedance percentage
1	75.7	0.0005
2	62.9	0.002
3	50.4	0.005
4	46.3	0.01
5	38.7	0.03
6	33.4	0.05
7	27.8	0.1
8	24.2	0.125
9	21.3	0.15

allow for quantification of longitudinal floodplain discharge ($m^3\ s^{-1}$), floodplain inundation areal extent (m^2), and floodplain inundation volume (m^3) at individual cross sections for specific discharge profiles. Individual cross section results were summed to estimate overbank values for each stream reach, as well as the entire main stem floodplain of Walnut Creek.

Suspended sediment and TP rating curves were developed using all available USDA-ARS stormflow grab sample data (n = 74) collected during event-based sampling at the watershed outlet stream gauging station between 2008 and 2017. The predictive equations were used to estimate SS and TP concentrations for all HEC-RAS discharge profiles. These concentrations were applied to floodplain inundation volumes to estimate flux of SS and TP from channel to floodplain for each discharge profile using the equation:

$$S_{fp} = \sum_{i=1}^{n} E\, c_i Q_i \left[\frac{Q_i - Q_t}{Q_i}\left(1 - \frac{w}{f}\right)\right] \quad (2)$$

where S_{fp} is mass flux to floodplain storage (Mg), n is number of discharge profiles, E is the floodplain trapping efficiency, c_i is concentration at discharge profile i (kg m^{-3}), Q_i is stream discharge at discharge profile i ($m^3\ s^{-1}$), Q_t as before is overbank threshold discharge ($m^3\ s^{-1}$), w is channel width (m) and f is width of inundated floodplain (m). To estimate the percentage of overbank flux that entered floodplain storage, a floodplain trapping efficiency component (E) was applied to all overbank SS and TP fluxes using the equation:

$$E = 1 - e^{\left(-\omega \times \left(\frac{A}{Q_i - Q_t}\right)\right)} \quad (3)$$

where, E is the floodplain trapping efficiency, ω is particle settling velocity (mm s^{-1}), and A is the areal extent of floodplain inundation (m^2). The estimate of trapping efficiency was based on the method introduced by Chen (1975), which has been successfully utilized in other floodplain sedimentation studies (Asselman and Van Wijngaarden, 2002; Narinesingh et al., 1999). Particle settling velocity was estimated using the relationship developed by Thonon et al. (2005):

$$\omega = aD^b, \quad (4)$$

where D is particle diameter (μm), and a (2.7×10^{-4}) and b (1.57) are constants. The Thonon equation was selected because it utilizes a single representative grain size. As suspended sediment grain size distribution data was unavailable at time of study, researchers used the Camp Creek median grain size (D_{50}) of 30 μm (Beck et al., 2018) as the representative suspended sediment grain size. As mentioned in Section 2.1.2, Camp Creek represents the uppermost stratigraphic floodplain unit. Although grain size distribution of deposited sediment may differ significantly from the grain size distribution of SS, the Camp Creek D_{50} was deemed the best available estimate for the current study. The selected representative grain size of 30 μm falls within a range that has been successfully used for the same purpose in other floodplain sedimentation studies (Asselman, 1999; Asselman and Van Wijngaarden, 2002; Middelkoop and Van der Perk, 1998). For this study, TP was assumed to move with SS, thus one value of E was utilized for both SS and TP.

To elucidate the effects of channel adjustment on floodplain inundation frequency and floodplain SS and TP storage, the series of discharge profiles were run in both the 1998 and 2014 HEC-RAS models. Model outputs were used to quantify longitudinal floodplain discharge ($m^3\ s^{-1}$), width of floodplain inundation (m), floodplain inundation areal extent (m^2), floodplain inundation volume (m^3), and the resulting SS and TP floodplain storage masses (Mg) for between-model comparisons. An out-of-bank flow event presented the opportunity for model verification in June, 2018. Following the event, researchers quantified areal flood extent for a 1.6 km (longitudinal) stream reach using handheld GPS, with physical flood evidence (e.g., debris accumulations, vegetation disturbance) as the basis for delineation. The June, 2018 areal extent boundary was then compared with HEC-RAS model results for an event of equal discharge (Fig. 11, Supplementary material).

2.4. Laboratory and statistical methods

Stormflow surface water samples were collected as grab samples at the watershed outlet stream gauging station by USDA-ARS staff and analyzed for SS and TP at the USDA-ARS National Laboratory for Agriculture and the Environment (NLAE). Analysis for SS was performed by whole sample gravimetric analysis (ASTM, 2000). Analysis for TP was performed using persulfate digestion, with P concentrations determined by colorimetric analysis using a spectrophotometer.

Simple linear regression and the Mann-Kendall trend test were performed on flow duration curve data to detect any temporal trends in the hydrologic regime (Helsel and Hirsch, 2002). Suspended sediment and TP rating curve predictive equations were developed using simple linear regression methods outlined in Rasmussen et al. (2011). Regression analysis utilized log (base 10) transformations of both explanatory (i.e., discharge) and response variables (i.e., SS, TP), as well as Duan's bias correction factor (Duan, 1983). Wilcoxon signed-rank tests were used to test for differences in overbank parameter outputs between the 1998 and 2014 models. All statistical procedures were performed using R v. 3.4.1 (R Core Team, 2017).

3. Results

3.1. Channel dimensions

Surveyed channel cross sectional area increased by 16.8% between 1998 and 2014, with the majority (76%) of cross sections exhibiting degradation and widening (Fig. 2). Change at individual cross section transects between 1998 and 2014 ranged from −12.8% (i.e., decrease in area) to >60% (Fig. 3). Mean cross section width (top bank) increased by 9.5% from 1998 (10.5 m) to 2014 (11.5 m), and mean depth to thalweg (i.e., distance from top bank to channel bed at thalweg) increased 9.4% from 1998 (2.71 m) to 2014 (2.97 m). Cross section mean width/depth ratio was nearly identical (~3.9) for both years, with 1998 ratios ranging from 2.71 to 7.75, and 2014 ratios ranging from 2.8 to 5.8. For both years, cross section characteristics of depth to thalweg, width, and cross sectional area generally increased with distance downstream (i.e., drainage contributing area). Width/depth ratio, however, exhibited no longitudinal spatial trend (i.e., systematic change in the upstream or downstream direction) during either year. Change in channel cross section characteristics (i.e., width, depth, width/depth ratio, and area) between 1998 and 2014 also lacked an observable spatial pattern.

3.2. Hydrology

Linear regression ($p < 0.001$, $b_1 = 3.61 \times 10^{-7}$) and Mann-Kendall ($\tau = 0.016$, $p < 0.001$) tests for trend indicate an increase in mean hourly discharge between years 1995 and 2017. In contrast, visual analysis of ~5-year period FDCs (Fig. 4) suggests lack of a systematic temporal trend in hydrologic regime between 1995 and 2017. In addition to the visual analysis suggesting no meaningful change in hydrologic regime between 1995 and 2017, the slope for the increase in threshold majority discharge between 1998 and 2014 (2.52×10^{-5}) was ~115 times greater than the mean hourly discharge slope detected in trend analyses.

The discharge-area relationship used to scale watershed outlet discharges to discharges at individual cross sections was validated using the upstream gauging station FDC, and included 18 upstream gauging station discharges ranging from 0.005 to 32.7 $m^3\ s^{-1}$ ($R^2 = 0.98$, RMSE = 2.7). Discharge-area predictions for the upstream gauging station location fell within 5.5% of gauge-measured mean discharges, and

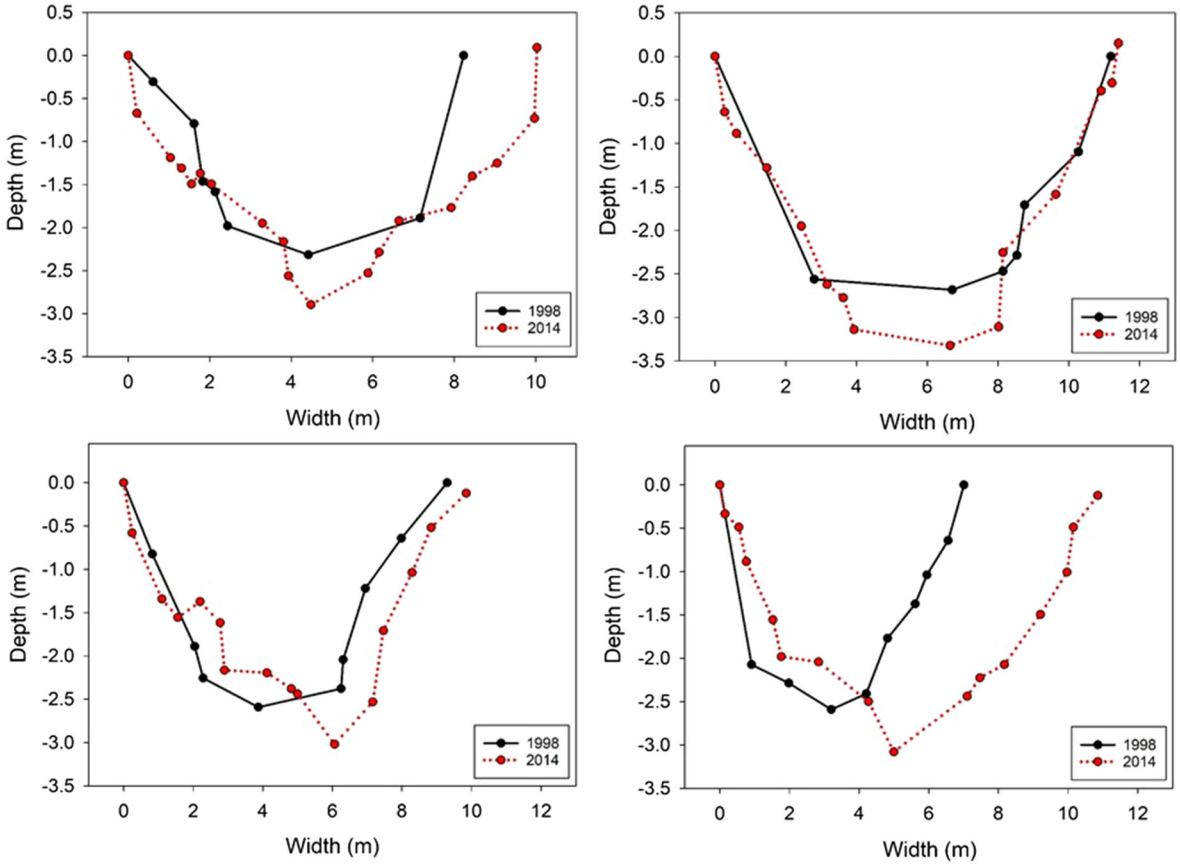

Fig. 2. Channel cross section dimensional change between 1998 and 2014 at a subset of study cross sections. Subset represents typical pattern of degradation and widening along main stem of Walnut Creek, Iowa. Left top banks (looking downstream) located at 0.0 m depth on Y axes.

thus the discharge-area scaling technique was determined to be an acceptable means of estimating cross section discharge.

3.3. Channel-floodplain lateral connectivity

3.3.1. Overbank threshold discharges

Bankfull threshold discharges were found to increase between 1998 and 2014 (Fig. 5). As described in Section 2.3.2, the overbank threshold discharge was defined as the discharge required to initially force streamflow to exit the channel and enter the floodplain on at least one side of the channel. Minimum discharge (i.e., mean hourly watershed outlet discharge at which only one cross section remains overbank) increased 28.9% between 1998 (14.9 $m^3\ s^{-1}$) and 2014 (19.2 $m^3\ s^{-1}$) (Fig. 6). Majority discharge (i.e., mean hourly watershed outlet discharge required to produce overbank flow at >50% of cross-sections) increased 14.9% between 1998 (24.2 $m^3\ s^{-1}$) and 2014 (27.8 $m^3\ s^{-1}$). Maximum discharge (i.e., mean hourly watershed outlet discharge required to produce overbank flow at 100% of cross sections) exhibited the lowest degree of change (12.9% increase) between 1998 (62.9 $m^3\ s^{-1}$) and 2014 (71.0 $m^3\ s^{-1}$).

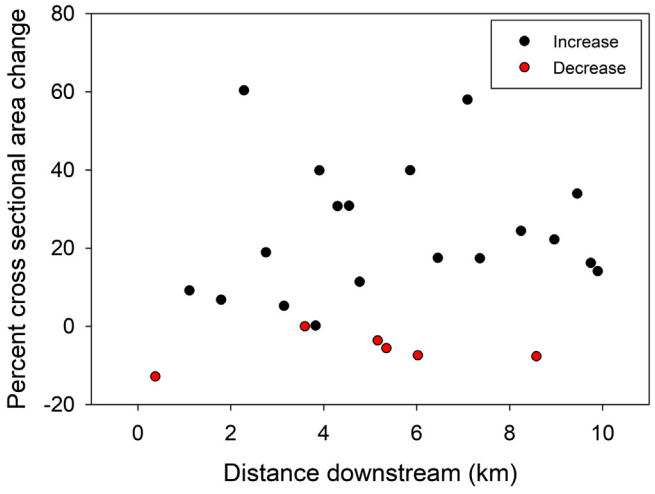

Fig. 3. Percent area change for individual channel cross sections between 1998 and 2014, Walnut Creek, Iowa.

The increase in threshold discharges represent shifts to lower (i.e., less frequent) threshold percent exceedances on the flow duration curve, with the majority discharge percent exceedance decreasing from 0.125% (1998) to 0.1% (2014) (Fig. 7). Minimum discharge percent exceedance decreased from 0.25 to 0.175% between 1998 and 2014, and maximum discharge percent exceedance decreased from 0.0021 to 0.0011% over the same time period.

3.3.2. Floodplain storage trends

Trends in floodplain storage were evaluated by comparing the individual HEC-RAS flow simulations of all discharge profiles. Floodplain inundation volume (m^3) outputs for the 1998 HEC-RAS model were >2014 model outputs (Fig. 8a.) for all discharge profiles (Table 1). Across all discharge profiles, main stem floodplain inundation volume ranged from 90 m^3 to 489,120 m^3 (mean = 156,738 m^3) for the 1998 model, and from 30 m^3 to 387,890 m^3 (mean = 98,460 m^3) for the 2014 model. This equates to a decrease of 58,278 m^3 (−37.2%) in mean volume between years. It should be noted that these values do not represent rates, but are individual data points used for comparison of overbank inundation between models. Predicted main stem floodplain inundation surface area (m^2) was also greater for the 1998

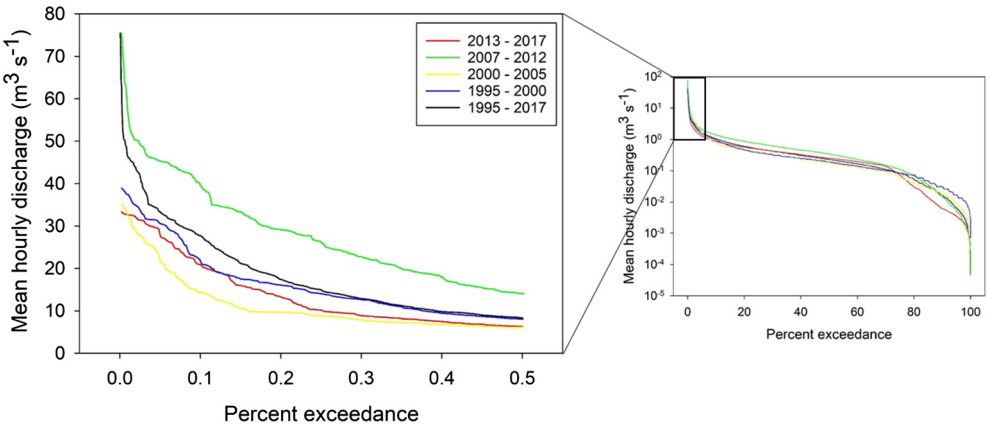

Fig. 4. Flow duration curves derived from watershed outlet mean hourly discharge data, Walnut Creek, Iowa. Black line represents curve for full data availability period, lines in color represent curves for ~5-year periods. Upper portions of curves at left.

model (Fig. 8b.), with outputs from all discharge profiles ranging from 2470 m^2 to 798,690 m^2 (mean = 315,833 m^2) compared to the range of 20 m^2 to 694,870 m^2 (mean = 205,084 m^2) for the 2014 model. This equates to a decrease of 110,749 m^2 (−35.1%) in mean surface area between years.

The proportions of the floodplain experiencing inundation at individual cross section transects (normalized by floodplain width) were found to be significantly greater in 1998 than in 2014, for the top 6 (i.e., low frequency) discharge profiles ($0.0005 < p < 0.05$) (Fig. 9). No significant difference was detected between 1998 and 2014 for the bottom 3 (i.e., most frequent) discharge profiles ($0.58 < p < 0.59$).

The 1998 model predicted greater watershed-scale flux of SS and TP to floodplain storage for all discharge profiles compared with the 2014 model (Fig. 10). For all discharge profiles, flux of SS to floodplain storage ranged from 9 Mg hr^{-1} to 2700 Mg hr^{-1} (mean = 950 Mg hr^{-1}) for the 1998 model, and from 0.07 Mg hr^{-1} to 2355 Mg hr^{-1} (mean = 659 Mg hr^{-1}) for the 2014 model (Fig. 10 a.). This equates to a decrease of 291 Mg hr^{-1} (−30%) in mean SS mass storage rate between years. Predicted TP flux to floodplain storage ranged from 7.5×10^{-3} to 1.7 Mg hr^{-1} (mean = 0.62 Mg hr^{-1}), and from 5×10^{-5} to 1.5 Mg hr^{-1} (mean = 0.42 Mg hr^{-1}) for the 1998 and 2014 models, respectively (Fig. 10b.). This equates to a decrease of 0.2 Mg hr^{-1} (−32%) in mean TP mass storage between years.

When estimated rates of floodplain storage were applied to all FDC discharges greater than respective overbank discharge thresholds, the 1998 model predicted an annual flux of 3787 Mg SS and 2.64 Mg TP to floodplain storage along the entire ~10 km of Walnut Creek's main stem. The 2014 model predicted annual fluxes of 1489 Mg (SS) and 1.0 Mg (TP), which represent decreases of ~61 and ~62% from 1998 estimations.

Mean model-estimated floodplain trapping efficiency (across all profiles) decreased ~7% between 1998 (44%) and 2014 (41%). Floodplain trapping efficiency (E) was calculated using Eq. (3), in which area (A) of floodplain inundation extent (m^2) is a significant driver of trapping efficiency.

4. Discussion

4.1. Channel adjustment

Walnut Creek's main stem increased in cross sectional area by an average of 16.8% (2.91 m^2) between 1998 and 2014, which equates to an

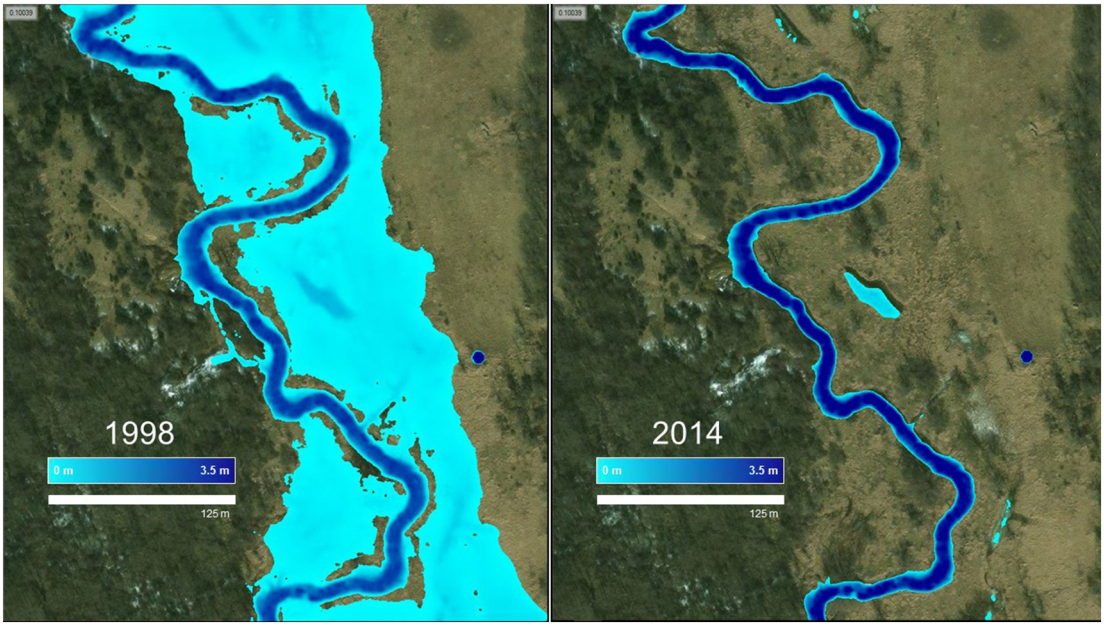

Fig. 5. Floodplain inundation extent and depth for the 1998 (left image) and 2014 (right image) models for the identical watershed outlet discharge of 27.75 m^3 s^{-1}. The depicted subreach is representative of the overall trend of decrease in channel-floodplain connectivity between 1998 and 2014. Blue gradient bar indicates flow depth.

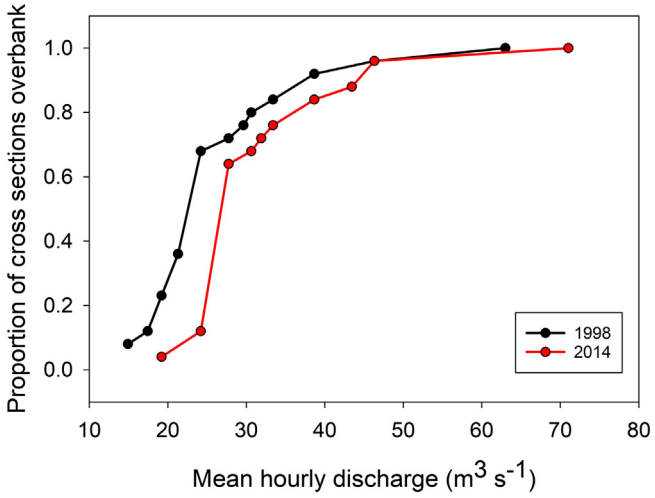

Fig. 6. Proportion of channel cross sections exhibiting overbank flow in 1998 and 2014, by watershed outlet discharge, Walnut Creek, Iowa.

average annual rate of ~1% (0.18 m^2 yr^{-1}). Width and depth mean annual increases were 0.06 and 0.02 m yr^{-1}, respectively. Although a limited number individual cross sections exhibited a decrease or negligible change in cross sectional area during that time period (Fig. 4), a clear pattern of degradation and widening is present along Walnut Creek's main stem.

Rates of channel dimensional change in Walnut Creek are lower than those reported in other loess-derived alluvial channels in the United States. Hamlett et al. (1983) reported a 43% increase (0.29 m^2 yr^{-1}) in channel cross sectional area over a 16 year period (1964–1980) in the Four Mile Creek watershed, Iowa. Four Mile Creek has similar land area (5050 ha), floodplain soils (alluvial silt and clay) and disturbance impact (land cover alteration, channelization) as Walnut Creek, however, cross sectional measurements in Four Mile occurred much closer, temporally, to its reported period of maximum channel disturbance (mid to late 1970s). It is of note that Four Mile Creek rates of change recorded prior (i.e., mid to late 1960s) to the period of maximum disturbance more closely resembled rates reported for Walnut Creek. In the Tarkio River watershed in western Iowa, (Simon and Rinaldi, 2013) reported 6–8 m of bed degradation over a period of ~100 years for loess derived alluvial channels, and an associated increase in channel width

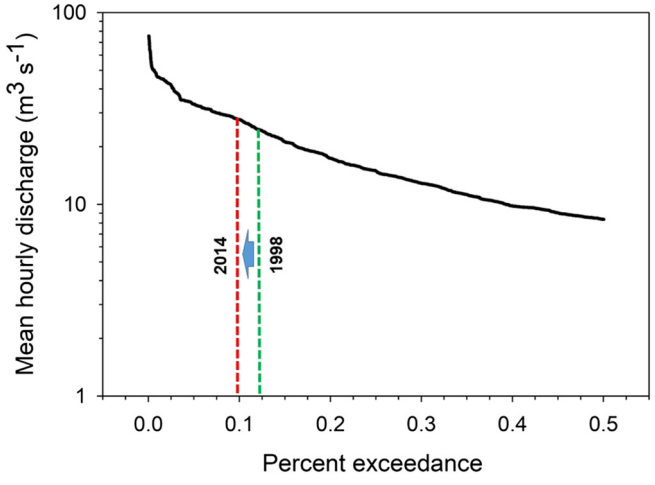

Fig. 7. Shift in threshold majority discharge percent exceedance between 1998 (green line) and 2014 (red line) on the watershed outlet flow duration curve (black line), Walnut Creek, Iowa.

of 31 m. Similar to Four Mile Creek, the greatest rates of channel change occurred in the period immediately following maximum disturbance, with subsequent non-linear decreases in rate with time. Simon (1989) reported mean channel widening rates of 0.17 to 2.2 m yr^{-1}, and a maximum bed degradation of 6.1 m for loess-derived alluvial channels in western Tennessee. These changes were observed approximately 5–24 years following the period of significant disturbance in study watersheds (i.e., wide spread channelization).

Rates of change in bed degradation in the Iowa and Tennessee studies follow a pattern of non-linear adjustment following disturbance (Schumm and Lichty, 1965; Graf, 1977). In other words, rates of change are greatest immediately following disturbance, and decrease non-linearly (i.e., power function) along an asymptote approaching critical stream power (b_1=0) as time from disturbance increases (Simon, 1989, Fig. 2). This pattern has been observed in a number of studies focused on channel response to disturbance (e.g., Williams and Wolman, 1984; Hadish et al., 1994; Heine and Lant, 2009). It should be noted that the pattern of non-linear adjustment is associated with bed degradation, and not overall increase in channel cross sectional area. However, bed degradation is the primary driver of channel evolution, and widening does not occur until a critical point of incision is reached (i.e., point where banks become too tall to remain stable). Thus, a link does exist between degradation and channel cross sectional area increase (i.e., combination of degradation and widening).

In light of this, time since disturbance could be one reason why Walnut Creek rates are lower than other studies conducted in loess-derived alluvial channels. Walnut Creek measurements occurred between 1998 and 2014, ~40 to 80 years following period of maximum disturbance. Schilling and Drobney (2014) hypothesized that downcutting of Walnut Creek into its floodplain probably began to occur soon after settlement, and an early report of Walnut Creek indicated that by 1905, the channel had already undergone "considerable downcutting" (Williams, 1905). Since cross section data pre-1998 are lacking for Walnut Creek, it may be assumed that the channel is currently within the near-zero slope region (i.e., b_1 approaching 0) of the non-linear adjustment curve and although change in channel dimension is apparent, it is occurring at lesser rates than studies that report results closer, temporally, to respective periods of maximum disturbance.

In addition, rates of channel adjustment may be impacted by the presence of the Gunder member. As mentioned in Section 2.1.2, the Gunder member represents the channel bed and streambank toe along a majority of Walnut Creek's length. The Gunder is characterized by a relatively high bulk density (1.6 g cm^{-3}) and a mean clay content of 21% (Beck et al., 2018). Gunder critical shear stress (i.e., threshold stress applied by flowing water required to initiate erosion) has been documented as ranging from 10.4 (Layzell and Mandel, 2014) to 34.8 Pa (Beck et al., unpublished hydraulic flume data). In addition, Thomas (2009) documented the Gunder as having a relatively high mechanical shear strength (i.e., threshold force required for material deformation), ranging from 435 to 711 Pa. Thus, the Gunder possesses an inherent degree of resistance to fluvial erosion. The erosion resistance may be enhanced further for channel bed Gunder, as permanent saturation from streamflow may nearly eliminate the freeze-thaw and wet-dry cycles that would weaken exposed Gunder (Hooke, 1979; Couper and Maddock, 2001). Thus, in Walnut Creek, the Gunder may act to regulate the degree of degradation and downcutting (Simon and Rinaldi, 2013), as opposed to Tarkio Creek and western Tennessee streams where deep loess deposits and lack of base level control promote unrestricted channel degradation. It is of note that Walnut Creek discharges to Red Rock reservoir approximately 10 km downstream of the watershed outlet gauging station, and thus a stabilized outlet elevation exists.

If Walnut Creek is in fact within the near-zero slope region of the non-linear adjustment curve, it may be further evidence for Stage IV of channel evolution (Simon, 1989). The assumption of Stage IV is supported by streambank angle (i.e., 70–90 degrees for vertical bank face, 25–50 degrees for upper bank), channel width/depth ratio (~3.9), and

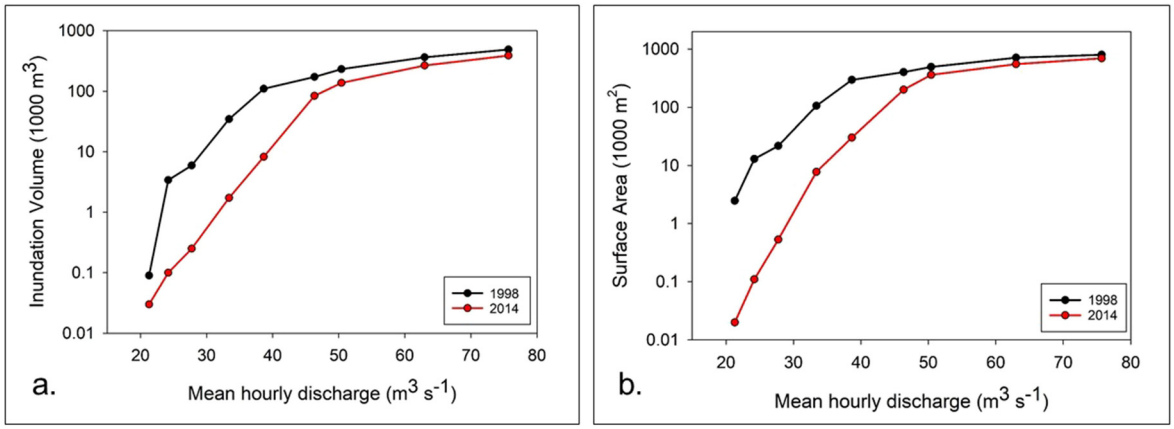

Fig. 8. Model-predicted inundation volume (a.) and surface area (b.) by discharge profile for the entire main-stem floodplain of Walnut Creek, Iowa. Individual data points represent results from individual HEC-RAS flow simulations. Mean hourly discharge is at watershed outlet.

channel change (i.e., degradation and widening) data as well as visual evidence from the watershed (i.e., mass wasting).

4.2. Channel-floodplain connectivity

A simplistic uniform flow analysis (Eq. (1)) was used to predict the relationship between the 1998 and 2014 threshold overbank discharges. Eq. (1) inputs of λ (1.096) and θ (1.095) were derived from field measurements of mean cross section depth and width change between 1998 and 2014. Using these field-derived inputs, Eq. (1) predicted the relationship between 1998 and 2014 threshold overbank discharges to be 1.27. In other words, using strictly Manning's equation and field measured data of cross section width and depth change, the threshold overbank discharge was predicted to increase by 27% between 1998 and 2014.

Using the same field data as inputs, HEC-RAS outputs predicted increases in minimum, majority, and maximum threshold discharges of 28, 15, and 13%, respectively, between 1998 and 2014. Compared with the Manning's results, HEC-RAS predicted smaller increases in maximum and majority threshold discharges between 1998 and 2014. These differences likely reflect non-uniform flow effects and highlight the value of numerical hydraulic models such as HEC-RAS for inundation and sedimentation studies.

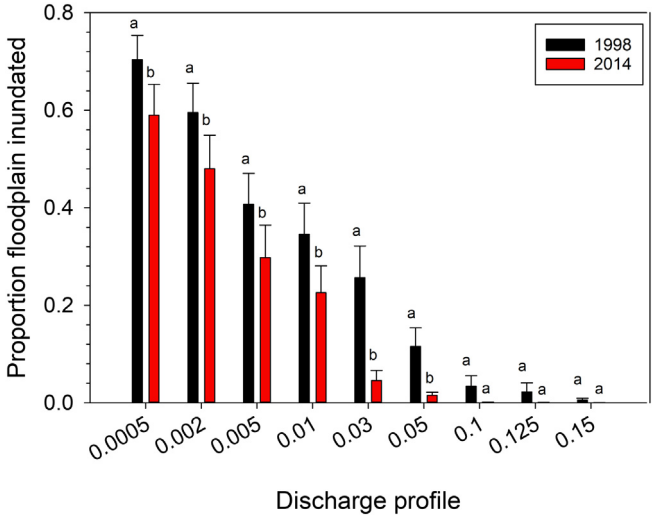

Fig. 9. Proportion of the floodplain experiencing inundation (normalized by floodplain width at cross section), by discharge profile. Difference in lower case letters for individual discharge profiles indicates significant difference at $\alpha = 0.05$.

In general, connectivity between Walnut Creek and its floodplain decreased between 1998 and 2014. In 2014, flow events of greater discharge, and thus lower frequency of occurrence, would be required to maintain the same degree of floodplain connection (i.e., inundation volume, areal extent, SS and TP flux) observed in 1998. The mean increase in channel cross sectional area of 2.91 m^2 over the 16 year period was associated with a number of model-predicted changes to channel-floodplain connectivity in the Walnut Creek watershed. The minimum, majority, and maximum overbank threshold discharges all increased in magnitude, and decreased in percent exceedance (i.e., became less frequent) as more water was able to be conveyed within the channel. Majority discharge, for example, increased at an average rate of 0.23 $m^3\ s^{-1}$ per year, while cross sectional area increased by an average of 0.18 m^2 per year. In 2014, the difference between majority discharge and minimum discharge was 8.54 $m^3\ s^{-1}$. Using annual rates of change for majority discharge (0.23 $m^3\ s^{-1}$) and cross sectional area (0.18 m^2), it would take an increase in channel cross section area of 6.72 m^2 to shift the 2014 majority discharge to the level of 2014 minimum discharge. At the current rate of channel enlargement (0.18 $m^2\ yr^{-1}$), ~37 years would be required for the current majority discharge (27.75 $m^3\ s^{-1}$) to become the minority discharge, at which ~50% of the Walnut Creek floodplain would lose connection with its channel for a significant portion of the flow regime (i.e., lower flows). Until large stretches of Walnut Creek's channel transition to stage V (aggradation), connectivity between the channel and floodplain will continue to decline.

For each observed 1 m^2 increase in channel area between 1998 and 2014, mean rate of SS flux to floodplain storage was observed to decrease by 100 Mg hr^{-1}, and mean rate of TP flux was observed to decrease by 0.07 Mg hr^{-1}. If instead of being diverted into floodplain storage, 100% of these SS and TP masses were exported from the watershed with streamflow, each 1 m^2 increase in channel area would increase watershed export of SS by 100 Mg hr^{-1}, and watershed export of TP by 0.07 Mg hr^{-1}. At the observed rate of channel enlargement (0.18 $m^2\ yr^{-1}$), it would take ~5.5 years for the channel cross sectional area to increase by 1 m^2.

Floodplain trapping efficiency decreased ~7% between 1998 and 2014. This may have been primarily driven by the observed decrease in floodplain inundation surface area between years. The method used to estimate floodplain trapping efficiency (Eq. (3)) is sensitive to areal extent of floodplain inundation (A). In 1998, flows inundated a greater proportion of the floodplain (i.e., larger A) (Fig. 9) with shallow water, which promoted sediment deposition. During 2014, however, flows lacked the inundation extent seen in 1998 (i.e., smaller A), and an increased proportion of flows (especially for lower discharges) were confined to the channel margin area. These flows were bound between natural levees with no opportunity to spread across the floodplain. While these flows were in fact overbank, their confinement to the

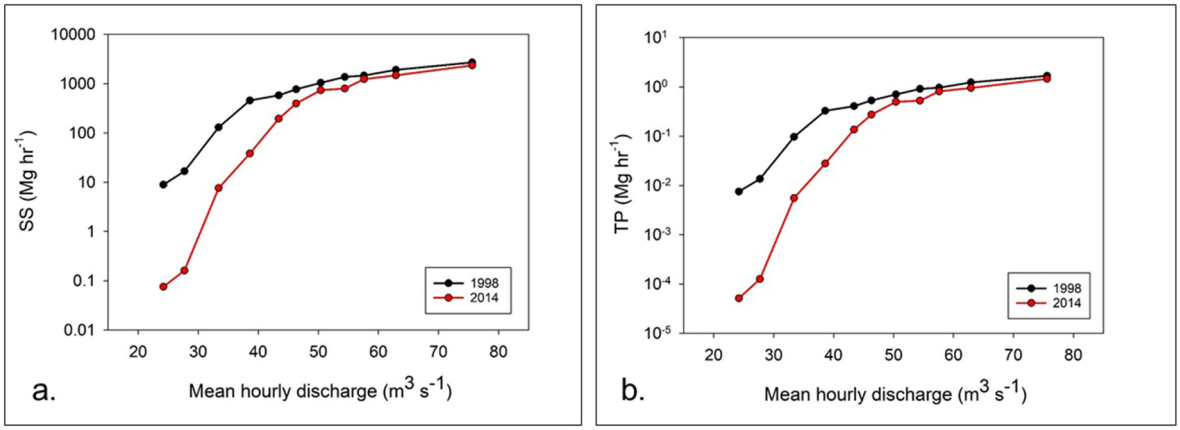

Fig. 10. Model-predicted SS (a.) and TP (b.) storage rates by discharge profile for the entire main-stem floodplain of Walnut Creek, Iowa. Individual data points represent results from individual HEC-RAS flow simulations. Mean hourly discharge is at watershed outlet.

channel margin resulted in lesser areal extent and higher velocities (i.e., conditions that reduce sediment settling) than flows observed in 1998.

A number of assumptions were made during this study, many of which may have influenced results. It should be restated that our HEC-RAS models were run under steady flow conditions (i.e., no change in discharge with time). Steady flow conditions are rare in the environment, however, as watersheds are continuously responding to inputs of precipitation and other hydrological factors. Because our models were run under steady flow conditions, we were unable to resolve discharge transients that would likely be important in the floodplain inundation pattern and sequence. Unsteady models driven with observed hydrographs could yield more spatial and temporal detail in overbank flow paths and flow depths, and may affect the extent and duration of overbank flows. The use of a steady model, however, provides an upper bound to the real extent. Moreover, since this idealization of the problem affects both the 1998 and 2014 model scenarios, the change in inundation extent over time should be less affected by the idealization. Furthermore, since our overall objective was to assess *change* in overbank frequency and volume accompanying channel change, the assumption of steady flow would be expected to have similar results in both 1998 and 2014 models. Steady state models are recognized as an appropriate tool for a range of watershed management efforts, notably flood risk assessment (Bales and Wagner, 2009; Gilles et al., 2012). Development of new utilizations of these practical tools addresses a great need for development of simplistic approaches to investigate and quantify channel-floodplain lateral connectivity at the watershed scale (Newson and Large, 2006; Soar et al., 2017), as well as watershed scale sediment and TP dynamics.

We used a single representative suspended sediment grain size to estimate floodplain trapping ability (Eqs. (3), (4)). The relationship between model-estimated floodplain storage and D_{50} was found to vary across a range of grain sizes (2 μm–250 μm). Floodplain storage sensitivity increased with decreases in D_{50}, with the greatest sensitivity observed within the fine silt range (i.e., 2–10 μm). Within the fine silt range, each 1 μm increase in D_{50} resulted in a >100% increase in floodplain storage. For the 20–60 μm range, however, each 1 μm increase in D_{50} only increased mass flux by an average of ~5%. As the 20–60 μm range is thought to be a realistic selection range for suspended sediment D_{50}, especially for studies such as this, D_{50} should be recognized as having slight to moderate impacts on storage results.

If a finer D_{50} (i.e., <30 μm) were selected, both models would have experienced decreases in SS mass flux to floodplain storage. However, the 2014 model would have seen a disproportionately greater effect, as observed flow characteristics (i.e., propensity of flows to be confined within channel margin and not spread over floodplain) did not promote settling of SS. Spatially, both models would have predicted greater accumulations of SS further (laterally) from the channel margin with a finer D_{50}. If a coarser D_{50} were selected (e.g., to more closely mimic the flocculated nature of suspended material), both models would have seen increases in SS mass flux to floodplain storage. For both models, the near channel area would experience increased SS deposition, as the shear zone and steep velocity gradient present in that area promotes settling of large particles. This may lead to the growth of natural levees.

Precipitation and discharge have increased within the Midwest U.S. over the past ~80 years (Andresen et al., 2012; Zhang and Schilling, 2006), and this trend may have implications for channel morphology. However, although trend analyses detected a minor increase in mean hourly discharge between 1995 and 2017, we assumed hydrology to be stationary for the purposes of this study. Although the 2007–2012 FDC data (green line, Fig. 4) include three exceptionally wet years (i.e., 2008, 2009, 2010), during which numerous mean hourly discharges >40 $m^3\ s^{-1}$ were recorded at the watershed outlet (<0.028% exceedance for 1995–2017 data period), visual analyses of FDC data indicate no systematic increase in discharge. In addition to the visual analysis suggesting no meaningful change in hydrologic regime between 1995 and 2017, the slope for the increase in threshold majority discharge between 1998 and 2014 (2.52×10^{-5}) was ~115 times greater than the mean hourly discharge slope detected in trend analyses. This suggests that the detected increase in streamflow most likely had a negligible impact on the change in channel conveyance, as compared to change in conveyance brought about by cross sectional area change. In addition, the regression analysis included all parts of the FDC, including baseflow. While it may be possible that the changes in lower magnitude flows, which have no chance of accessing the floodplain, account for the statistical trend, they can't account for the top of bank threshold discharge brought about by cross sectional area change accompanying channel evolution.

Lastly, we assumed that 100% of stormflow TP occurred as particulate-P, and thus depositional mechanisms of TP would be identical to those of SS. While dissolved P (i.e., orthophosphate) has been documented as being a significant contributor to the annual TP loads of Iowa watersheds (Schilling et al., 2017), we would expect particulate-P to be the dominant contributor to stormflow TP (Gentry et al., 2007), especially during events large enough to produce overbank flow (Sharpley et al., 2008). The assumption of particulate-P dominance in Walnut Creek storm flow is supported by unpublished grab sample data collected at the watershed outlet, where orthophosphate represented, on average, ~19% of storm flow TP. It is not unreasonable to assume that a large proportion of dissolved-P in overbank flow would not be trapped on the floodplain, but instead reenter the channel with flow at points downstream. Thus, if we were to account for dissolved-P

contributions to TP, mass flux of TP to floodplain storage would be expected to decrease for both models.

4.3. Implications

Previously reported annual loads of SS at the Walnut Creek watershed outlet gauging station (Fig. 1) have ranged from 2625 to 16,693 Mg for calendar years 1998 through 2000 (May et al., 1999; Nalley et al., 2000; Nalley et al., 2001; Nalley et al., 2002), and from 6172 to 25,815 Mg for calendar years 2005 through 2011 (Palmer et al., 2014). Schilling et al. (2006) reported annual loads of TP that ranged from 1.7 to 9.0 Mg for calendar years 2000–2005.

As reported in Section 3.3.2, HEC-RAS predicted reductions in annual overbank floodplain storage of 2298 Mg (SS) and 1.63 Mg (TP) between the 1998 and 2014 models. These masses would no longer enter the floodplain storage pool, and would remain confined to the channel, where they may exit the watershed and contribute to watershed SS and TP export. If we consider the maximum reported annual loads of SS (25,815 Mg) and TP (9 Mg), the estimated reduction in export due to change in floodplain storage may increase SS and TP export by ~9 and 18%, respectively. In addition to loss of storage, higher discharges confined to the channel may have greater stream power, resulting in further enhancement of SS and TP export through accelerated bank and bed erosion.

For the main stem of Walnut Creek, streambank erosion contributions to SS loads have been documented for the years 2005–2011 (Palmer et al., 2014). Over study duration, streambank erosion contributions of SS ranged from −151 (i.e., accretion on banks) to 9921 Mg yr^{-1} (mean = 5299 Mg yr^{-1}). In addition, Beck et al. (2018) estimated streambank contributions of both SS and TP between May 2015 and May 2017. Streambank erosion contributions of SS were 2900 and 860 Mg for the first and second years, respectively, while contributions of TP were 0.65 and 0.23 Mg, respectively. For most years, annual estimated fluxes of SS to floodplain storage were less than streambank contributions. From these results, it can be assumed that the floodplain along Walnut Creek's main stem generally acts as a net source of SS to streamflow, and this source will increase further as channel evolution progresses.

The reduction in overbank storage provides a "1–2 punch" for watershed export, as both a storage opportunity is lost and stream power is increased. In addition, the resulting increases to watershed SS and TP export from in-channel sources may mask water quality improvements derived from edge-of-field and in-field conservation practices (Walling, 1983; Trimble and Crosson, 2000). This "1–2 punch" may be mitigated to some extent by implementing in-channel practices that act to reduce conveyance and enhance the channel-floodplain connection (e.g., reintroduced meandering, in-channel large wood, increased beaver (*Castor canadensis*) populations). The authors are aware, however, of the challenges these potential mitigation strategies may present in agricultural regions.

5. Conclusions

This study combined channel cross section field measurements with HEC-RAS modeling to investigate changes in floodplain inundation and storage within the context of channel geometry change in Walnut Creek, Iowa. Field observations indicate a 16.8% increase in channel cross sectional area over a 16 year period (1998–2014). Model results suggest that the increase in channel cross sectional area was associated with increases in overbank discharge thresholds (i.e., discharges required to force flow to exit channel and enter floodplain), significant decreases in annual floodplain inundation volume and areal extent, as well as decreases in annual fluxes of SS and TP to floodplain storage of ~61 and ~62%, respectively.

The modeled reduction in floodplain storage potential with a growing channel cross section may have significant implications on SS and TP loads exiting the Walnut Creek watershed. Estimated reductions in annual floodplain storage between the 1998 and 2014 models may represent an apparent increased contribution to annual SS and TP watershed export of ~9 to 18%, respectively. In addition, reduction in floodplain inundation results in a greater volume of water confined to the channel during flow events. The resulting increase in stream power may accelerate bed and bank erosion, further contributing to SS and TP export.

Cross section data (e.g., dimensional change, bank angles) and field observation of processes (i.e., mass wasting) indicate that the main stem of Walnut Creek is predominately in stage IV (i.e., degradation and widening) of channel evolution. Thus, the degree and frequency of floodplain inundation, as well as flux of SS and TP to floodplain storage are expected to decrease further as the channel continues to degrade and widen in progression towards stages V and VI. Contributions to watershed loads from loss of floodplain storage opportunities, and potentially increased bed and bank contributions from increased stream power, may mask SS and TP reductions achieved through edge of field practices. Because of these factors, it is critical that stage and progression of channel evolution be taken into consideration when addressing sediment and phosphorus loading at the watershed scale.

Supplementary data to this article can be found online at https://doi.org/10.1016/j.scitotenv.2019.01.038.

Acknowledgements

This project was supported by the Agriculture and Food Research Initiative (AFRI), Competitive Grant # 2013-67019-21393, from the United States Department of Agriculture National Institute of Food and Agriculture. The authors thank the United States Department of Agriculture, Agricultural Research Service, National Laboratory for Agriculture and the Environment, Ames, IA, USA staff for providing water quality and quantity data and associated analyses pertinent to this study. The authors thank Andrew Craig P.E., and Dr. Michelle Soupir, Department of Agricultural and Biosystems Engineering, Iowa State University, for hydraulic flume expertise and access. The authors thank Pauline Drobney, United State Fish and Wildlife Service, Department of Interior, Neal Smith National Wildlife Refuge, for providing access to field study sites.

Statement of conflict of interest

The authors have no conflict of interest to declare.

References

Allen, S.T., Krauss, K.W., Cochran, J.W., King, S.L., Keim, R.F., 2016. Wetland tree transpiration modified by river-floodplain connectivity. J. Geophys. Res. Biogeosci. 121, 753–766. https://doi.org/10.1002/2015JG003208.

Andresen, J., Hilberg, S., Kunkel, K., 2012. Historical Climate and Climate Trends in the Midwestern USA. White Pap. Prep. U.S. Glob. Chang. Res. Progr. Natl. Clim. Assess. Midwest Tech. Input Rep.

Arcement, G.J., Schneider, V.R., 1989. Guide for selecting Manning's roughness coeffients for natural channels and flood plains. USGS Water supply paper 2339. Area 2339, 39. https://doi.org/ReportNo.FHWA-TS-84-204.

Asselman, N.E.M., 1999. Grain-size trends used to assess the effective discharge for floodplain sedimentation, River Waal, the Netherlands. J. Sediment. Res. 69, 51–61. https://doi.org/10.2110/jsr.69.51.

Asselman, N.E.M., Van Wijngaarden, M., 2002. Development and application of a 1D floodplain sedimentation model for the River Rhine in the Netherlands. J. Hydrol. 268, 127–142. https://doi.org/10.1016/S0022-1694(02)00162-2.

ASTM, 2000. Standard test methods for determining sediment concentration in water samples. D3977-97. West Conshohocken, PA.

Baker, V.R., 1977. Stream-channel responses to floods, with examples from central Texas. Geol. Soc. Am. Bull. 88, 1057–1071. https://doi.org/10.1130/0016-7606(1977)88<1057.

Bales, J.D., Wagner, C.R., 2009. Sources of uncertainty in flood inundation maps. J. Flood Risk Manage. 2, 139–147. https://doi.org/10.1111/j.1753-318X.2009.01029.x.

Batzer, D.P., Noe, G.B., Lee, L., Galatowitsch, M., 2018. A floodplain continuum for Atlantic coast rivers of the Southeastern US: predictable changes in floodplain biota along a river's length. Wetlands 38, 1–13. https://doi.org/10.1007/s13157-017-0983-4.

Beck, W., Isenhart, T., Moore, P., Schilling, K., Schultz, R., Tomer, M., 2018. Streambank alluvial unit contributions to suspended sediment and total phosphorus loads, walnut Creek, Iowa, USA. Water (Switzerland) 10. https://doi.org/10.3390/w10020111.

Belmont, P., Gran, K.B., Schottler, S.P., Wilcock, P.R., Day, S.S., Jennings, C., Lauer, J.W., Viparelli, E., Willenbring, J.K., Engstrom, D.R., Parker, G., 2011. Large shift in source of fine sediment in the upper Mississippi River. Environ. Sci. Technol. 45, 8804–8810. https://doi.org/10.1021/es2019109.

Bettis, E.A., 1990. The DeForest Formation of Western Iowa: Lithologic Properties, Stratigraphy, and Chronology. Iowa Department of Natural Resources, Des Moines, IA.

Bettis, E.A., Baker, R.G., Green, W.R., Whelan, M.K., Benn, D.W., 1992. Late Wisconsin and Holocene Alluvial Stratigraphy, Paleoecology, and Archaeological Geology of East-Central Iowa: Guidebook Series No. 12.

Biedenharn, D.S., Copeland, R.R., Thorne, C.R., Soar, P.J., Hey, R.D., Watson, C.C., 2000. Effective Discharge Calculation: A Practical Guide. Prepared for USACE.

Brunner, G.W., 2016. HEC-RAS river Analysis System User's Manual Version 5.0. USACE.

Chen, C.N., 1975. Design of sediment retention basins. National symposium on urban hydrology and sediment control, pp. 285–298 (Lexington, KY).

Couper, P.R., Maddock, I.P., 2001. Subaerial river bank erosion processes and their interaction with other bank erosion mechanisms on the River Arrow, Warwickshire, UK. Earth Surf. Process. Landf. 26, 631–646. https://doi.org/10.1002/esp.212.

Duan, N., 1983. A nonparametric smearing estimate: method retransformation. J. Am. Stat. Assoc. 78, 605–610.

Duvall, A., 2004. Tectonic and lithologic controls on bedrock channel profiles and processes in coastal California. J. Geophys. Res. 109, F03002. https://doi.org/10.1029/2003JF000086.

Forshay, K.J., Stanley, E.H., 2005. Rapid nitrate loss and denitrification in a temperate river floodplain. Biogeochemistry 75, 43–64. https://doi.org/10.1007/s10533-004-6016-4 (n.d.).

Gentry, L.E., David, M.B., Royer, T.V., Mitchell, C.A., Starks, K.M., 2007. Phosphorus transport pathways to streams in tile-drained agricultural watersheds. J. Environ. Qual. 36, 408. https://doi.org/10.2134/jeq2006.0098.

Gilles, D., Young, N., Schroeder, H., Piotrowski, J., Chang, Y.J., 2012. Inundation mapping initiatives of the Iowa flood center: statewide coverage and detailed urban flooding analysis. Water (Switzerland) 4, 85–106. https://doi.org/10.3390/w4010085.

Graf, L., 1977. The rate law in fluvial geomorphology. Am. J. Sci. 277, 178–191. https://doi.org/10.2475/ajs.277.2.178.

Griffith, G.E., Omernik, J.M., Wilton, T.F., Pierson, S.M., 1994. Ecoregions and subregions of Iowa: a framework for water quality assessment and management. J. Iowa Acad. Sci. 101.

Hadish, G.A., Braster, M., Lohnes, R.A., Baumel, C.P., 1994. Iowa DOT HR-352 Submitted to: Iowa Department of Transportation, Highway Division Submitted by: Golden Hills Resource Conservation and Development, Oakland Iowa.

Hamlett, J.M., Baker, J.L., Johnson, H.P., 1983. Channel morphology changes and sediment yield for a small agricultural watershed in Iowa. Am. Soc. Agric. Eng. 1390–1396.

Heine, R.A., Lant, C.L., 2009. Spatial and temporal patterns of stream channel incision in the loess region of the Missouri river. Ann. Assoc. Am. Geogr. 99, 231–253. https://doi.org/10.1080/00045600802685903.

Helsel, D., Hirsch, R., 2002. Statistical methods in water resources. US Geological Survey http://water.usgs.gov/pub/twri/twri4a3/.

Hooke, J.M., 1979. An analysis of the processes of river bank erosion. J. Hydrol. 42, 39–62. https://doi.org/10.1016/0022-1694(79)90005-2.

Hopkins, K.G., Noe, G.B., Franco, F., Pindilli, E.J., Gordon, S., Metes, M.J., Claggett, P.R., Gellis, A.C., Hupp, C.R., Hogan, D.M., 2018. A method to quantify and value floodplain sediment and nutrient retention ecosystem services. J. Environ. Manag. 220, 65–76. https://doi.org/10.1016/j.jenvman.2018.05.013.

Junk, W., Bayley, P.B., Sparks, R.E., 1989. The flood pulse concept in river-floodplain systems. In: Dodge, D.P. (Ed.), Proceedings of the International Large River Symposium (LARS). 106. Canadian Special Publication of Fisheries and Aquatic Sciences, pp. 110–127.

Kaase, C.T., Kupfer, J.A., 2016. Sedimentation patterns across a Coastal Plain floodplain: the importance of hydrogeomorphic influences and cross-floodplain connectivity. Geomorphology 269, 43–55. https://doi.org/10.1016/j.geomorph.2016.06.020.

Knox, J.C., 1977. Historical valley floor sedimentation in the Upper Mississippi Valley. Ann. Am. Assoc. Geogr. 77, 224–244.

Knox, J.C., 1987. Human impacts on Wisconsin stream channels. Ann. Am. Assoc. Geogr. 67, 323–342.

Knox, J.C., 2006. Floodplain sedimentation in the upper Mississippi Valley: natural versus human accelerated. Geomorphology 79, 286–310. https://doi.org/10.1016/j.geomorph.2006.06.031.

Kondolf, G.M., Piégay, H., Landon, N., 2002. Channel response to increased and decreased bedload supply from land use change: contrasts between two catchments. Geomorphology 45, 35–51.

Kronvang, B., Andersen, I.K., Hoffmann, C.C., Pedersen, M.L., Ovesen, N.B., Andersen, H.E., 2007. Water exchange and deposition of sediment and phosphorus during inundation of natural and restored lowland floodplains. Water Air Soil Pollut. 181, 115–121. https://doi.org/10.1007/s11270-006-9283-y.

Lane, S.N., Tayefi, V., Reid, S.C., Yu, D., Hardy, R.J., 2007. Interactions between sediment delivery, channel change, climate change and flood risk in a temperate upland environment. Earth Surf. Process. Landf. 32, 429–446. https://doi.org/10.1002/esp.1404.

Layzell, A.L., Mandel, R.D., 2014. An assessment of the erodibility of Holocene lithounits comprising streambanks in northeastern Kansas, USA. Geomorphology 213, 116–127. https://doi.org/10.1016/J.GEOMORPH.2014.01.003.

Lecce, S.A., 1997. Spatial patterns of historical overbank sedimentation and floodplain evolution, Blue river, Wisconsin. Geomorphology 18, 265–277. https://doi.org/10.1016/S0169-555X(96)00030-X.

Linhart, S.M., Nania, J.F., Sander Jr., C.L., Archfield, S.A., 2012. Computing daily mean streamflow at ungaged locations in Iowa by using the Flow Anywhere and flow duration curve transfer statistical methods. US Geol. Surv. Sci. Investig. Rep. 50.

Magilligan, F.J., 1985. Historical floodplain sedimentation in the Galena River Basin, Wisconsin and Illinois. Ann. Assoc. Am. Geogr. 75, 583–594. https://doi.org/10.1111/j.1467-8306.1985.tb00095.x.

May, B.J.E., Gorman, J.G., Goodrich, R.D., Miller, V.E., Turco, M.J., Linhart, S.M., 1999. Water Resources Data, Iowa, Water Year 1998: Surface Water - Mississippi River Basin. USGS-WRD-IA-98-1.

Middelkoop, H., Van Der Perk, M., 1998. Modelling spatial patterns of overbank sedimentation on embanked floodplains. Geogr. Ann. Ser. B 80, 95–109.

Midgley, T.L., Fox, G.A., Heeren, D.M., 2012. Evaluation of the bank stability and toe erosion model (BSTEM) for predicting lateral retreat on composite streambanks. Geomorphology 145–146, 107–114. https://doi.org/10.1016/j.geomorph.2011.12.044.

Moody, J.A., Pizzuto, J.E., Meade, R.H., 1999. Ontogeny of a flood plain Ontogeny of a flood plain. GSA Bull. 111, 291–303. https://doi.org/10.1130/0016-7606(1999)111<0291.

Nalley, G.M., Gorman, J.G., Goodrich, R.D., Miller, V.E., Turco, M.J., Linhart, S.M., 2000. Water Resources Data, Iowa, Water Year 1999, 1: Surface Water - Mississippi River Basin. USGS-WRD-IA-99-1.

Nalley, G.M., Gorman, J.G., Goodrich, R.D., Miller, V.E., Turco, M.J., Linhart, S.M., 2001. Water Resources Data, Iowa, Water Year 2000, 1: Surface Water - Mississippi River Basin. USGS-WRD-IA-00-1.

Nalley, G.M., Gorman, J.G., Goodrich, R.D., Miller, V.E., Turco, M.J., Linhart, S.M., 2002. Water Resources Data, Iowa, Water Year 2001, 1: Surface Water - Mississippi River Basin. USGS-WRD-IA-01-1.

Narinesingh, P., Klaassen, G.J., Ludikhuize, D., 1999. Floodplain sedimentation along extended river reaches. J. Hydraul. Res. 37, 827–845. https://doi.org/10.1080/00221689909498514.

Newson, M.D., Large, A.R.G., 2006. 'Natural' rivers, 'hydromorphological quality' and river restoration: a challenging new agenda for applied fluvial geomorphology. Earth Surf. Process. Landf. 31, 1606–1624. https://doi.org/10.1002/esp.1430.

Nicholas, A.P., Walling, D.E., Sweet, R.J., Fang, X., 2006. Development and evaluation of a new catchment-scale model of floodplain sedimentation. Water Resour. Res. 42. https://doi.org/10.1029/2005WR004579.

Noe, G.B., Hupp, C.R., 2009. Retention of riverine sediment and nutrient loads by coastal plain floodplains. Ecosystems 12, 728–746. https://doi.org/10.1007/s10021-009-9253-5.

Orr, C.H., Stanley, E.H., Wilson, K.A., Finlay, J.C., 2007. Effects of restoration and reflooding on soil denitrification in a leveed midwestern floodplain. Ecol. Appl. 17, 2365–2376. https://doi.org/10.1890/06-2113.1.

Palmer, J.A., Schilling, K.E., Isenhart, T.M., Schultz, R.C., Tomer, M.D., 2014. Streambank erosion rates and loads within a single watershed: bridging the gap between temporal and spatial scales. Geomorphology https://doi.org/10.1016/j.geomorph.2013.11.027.

Phelps, Q.E., Tripp, S.J., Herzog, D.P., Garvey, J.E., 2015. Temporary connectivity: the relative benefits of large river floodplain inundation in the lower Mississippi River. Restor. Ecol. 23, 53–56. https://doi.org/10.1111/rec.12119.

Pinay, G., Black, V.J., Planty-Tabacchi, A.M., Gumiero, B., Décamps, H., 2000. Geomorphic control of denitrification in large river floodplain soils. Biogeochemistry 50, 163–182. https://doi.org/10.1023/A:1006317004639.

R Core Team, 2017. R: A Language and Environment for Statistical Computing. R Foundation for Statistical Computing, Vienna, Austria.

Rasmussen, P.P., Gray, J.R., Glysson, G.D., Ziegler, A.C., 2011. Guidelines and procedures for computing time-series suspended sediment concentrations and loads from in-stream turbidity-sensor and streamflow data: U.S. Geological Survey techniques and methods book 3. chap. C4. (53 p.). https://pubs.usgs.gov/tm/tm3c4/.

Raven, E.K., Lane, S.N., Bracken, L.J., 2010. Understanding sediment transfer and morphological change for managing upland gravel-bed rivers. Prog. Phys. Geogr. 34, 23–45. https://doi.org/10.1177/0309133309355631.

Reid, L.M., Dunne, T., 2003. Sediment budgets as an organizational framework in fluvial geomorphology. In: Kondolf, M.G., Piégay, H. (Eds.), Tools in Fluvial Geomorphology. Wiley, New York, pp. 463–500.

Ruhlman, M.B., Nutter, W.L., 1999. Channel morphology evolution and overbank flow in the Georgia Piedmont. J. Am. Water Resour. Assoc. 35 (277-209).

Schilling, K.E., Drobney, P., 2014. Hydrologic recovery with prairie restoration at Neal Smith National Wildlife Refuge, Jasper County, Iowa. Miscellaneous Publication MP-48. Iowa Geological Survey, Iowa City, IA.

Schilling, K.E., Thompson, C.A., 2000. Walnut Creek watershed monitoring project, Iowa monitoring water quality in response to prairie restoration. J. Am. Water Resour. Assoc. 36, 1101–1114. https://doi.org/10.1111/j.1752-1688.2000.tb05713.x.

Schilling, K.E., Wolter, C.F., 2000. Application of GPS and GIS to map channel features in Walnut Creek, Iowa. J. Am. Water Resour. Assoc. 36, 1423–1434. https://doi.org/10.1111/j.1752-1688.2000.tb05737.x.

Schilling, K.E., Hubbard, T., Luzier, J., Spooner, J., 2006. Iowa Geological Survey Walnut Creek Watershed Restoration and Water Quality Monitoring Project: Final Report. Iowa Department of Natural Resources, IA.

Schilling, K.E., Palmer, J.A., Bettis, E.A., Jacobson, P., Schultz, R.C., Isenhart, T.M., 2009. Vertical distribution of total carbon, nitrogen and phosphorus in riparian soils of Walnut Creek, southern Iowa. Catena 77, 266–273. https://doi.org/10.1016/j.catena.2009.02.006.

Schilling, K.E., Isenhart, T.M., Palmer, J.A., Wolter, C.F., Spooner, J., 2011. Impacts of land-cover change on suspended sediment transport in two agricultural watersheds1. J. Am. Water Resour. Assoc. 47, 672–686. https://doi.org/10.1111/j.1752-1688.2011.00533.x.

Schilling, K.E., Kim, S.-W., Jones, C.S., Wolter, C.F., 2017. Orthophosphorus contributions to total phosphorus concentrations and loads in agricultural watersheds. J. Environ. Qual. 46, 828. https://doi.org/10.2134/jeq2017.01.0015.

Schumm, S.A., Lichty, R.W., 1965. Time, space, and causality in geomorphology. Am. J. Sci. https://doi.org/10.2475/ajs.263.2.110.

Schumm, S.A., Harvey, M.D., Watson, C.C., 1984. Incised Channels, Morphology, Dynamics and Control. Water Resources Publications, Littleton, Colorado.

Sear, D.A., Newson, M.D., Brookes, A., 1995. Sediment-related river maintenance: the role of fluvial geomorphology. Earth Surf. Process. Landf. 20, 629–647. https://doi.org/10.1002/esp.3290200706.

Sharpley, A.N., Kleinman, P.J.A., Heathwaite, A.L., Gburek, W.J., Folmar, G.J., Schmidt, J.P., 2008. Phosphorus loss from an agricultural watershed as a function of storm size. J. Environ. Qual. 37, 362. https://doi.org/10.2134/jeq2007.0366.

Simon, A., 1989. A model of channel response in disturbed alluvial channels. Earth Surf. Process. Landf. 14, 11–26. https://doi.org/10.1002/esp.3290140103.

Simon, A., Rinaldi, M., 2013. Incised Channels: Disturbance, Evolution and the Roles of Excess Transport Capacity and Boundary Materials in Controlling Channel Response. Treatise Geomorphol. 9, pp. 574–594. https://doi.org/10.1016/B978-0-12-374739-6.00255-4.

Soar, P.J., Wallerstein, N.P., Thorne, C.R., 2017. Quantifying river channel stability at the basin scale. Water (Switzerland) 9, 1–31. https://doi.org/10.3390/w9020133.

Stark, C.P., 2006. A self-regulating model of bedrock river channel geometry. Geophys. Res. Lett. 33, 1–5. https://doi.org/10.1029/2005GL023193.

Surian, N., Rinaldi, M., 2003. Morphological Response to River Engineering and Management in Alluvial Channels in Italy. https://doi.org/10.1016/S0169-555X(02)00219-2 (n.d.).

Thomas, J.T., 2009. Knickpoint Migration in Western Iowa. (M.S. thesis). University of Iowa, Iowa City, IA.

Thonon, I., Roberti, J.R., Middelkoop, H., van der Perk, M., Burrough, P.A., 2005. In situ measurements of sediment settling characteristics in floodplains using a LISST-ST. Earth Surf. Process. Landf. 30, 1327–1343. https://doi.org/10.1002/esp.1239.

Tockner, K., Stanford, J.A., 2002. Riverine flood plains: present state and future trends. Environ. Conserv. 29, 308–330. https://doi.org/10.1017/S037689290200022X.

Tockner, K., Pennetzdorfer, D., Reiner, N., Schiemer, F., Ward, J.V., 1999. Hydrological connectivity, and the exchange of organic matter and nutrients in a dynamic river floodplain system (Danube, Austria). Freshw. Biol. 41, 521–535.

Trimble, S.W., 1983. A sediment budget for Coon Creek basin in the Driftless Area, Wisconsin, 1853–1977. Am. J. Sci. https://doi.org/10.2475/ajs.283.5.454.

Trimble, S.W., Crosson, P., 2000. U.S. erosion rates: myth and reality. Science 289, 248–250.

Tufekcioglu, M., Isenhart, T.M., Schultz, R.C., Bear, D.A., Kovar, J.L., Russell, J.R., 2012. Stream bank erosion as a source of sediment and phosphorus in grazed pastures of the Rathbun Lake Watershed in southern Iowa, United States. J. Soil Water Conserv. 67, 545–555. https://doi.org/10.2489/jswc.67.6.545.

Venterink, H.O., Wiegman, F., Van der Lee, G.E.M., Vermaat, J.E., 2003. Role of active floodplains for nutrient retention in the River Rhine. J. Environ. Qual. 32, 1430. https://doi.org/10.2134/jeq2003.1430.

Vogel, R.M., Fennessay, N.M., 1994. Flow duration curves I: new interpretation and confidence intervals. J. Water Res. Pl. ASCE. 120, 485–504.

Walling, D.E., 1983. The sediment delivery problem. J. Hydrol. 65, 209–237.

Walling, D.E., Owens, P.N., Leeks, G.J.L., 1998. The role of channel and floodplain storage in the suspended sediment budget of the River Ouse, Yorkshire, UK. Geomorphology 22, 225–242. https://doi.org/10.1016/S0169-555X(97)00086-X.

Wasson, R., Mazari, R., Starr, B., Clifton, G., 1998. The recent history of erosion and sedimentation on the Southern Tablelands of southeastern Australia: sediment flux dominated by channel incision. Geomorphology 24, 291–308. https://doi.org/10.1016/S0169-555X(98)00019-1.

Willett, C.D., Lerch, R.N., Schultz, R.C., Berges, S.A., Peacher, R.D., Isenhart, T.M., 2012. Streambank erosion in two watersheds of the Central Claypan Region of Missouri, United States. J. Soil Water Conserv. 67, 249–263. https://doi.org/10.2489/jswc.67.4.249.

Williams, I.A., 1905. Geology of Jasper County. Iowa Geological Survey Volume XV, Annual Report, 1904. Iowa Geological Survey, Iowa City, IA.

Williams, G.P., Wolman, M.G., 1984. Downstream effects of dams on alluvial rivers. U.S. Geol. Surv. Prof. Pap. 1286. https://doi.org/10.1126/science.277.5322.9j.

Woltemade, C.J., 1994. Form and process: fluvial geomorphology and flood-flow interaction, Grant River, Wisconsin. Ann. Assoc. Am. Geogr. 84, 462–479. https://doi.org/10.1111/j.1467-8306.1994.tb01870.x.

Zaimes, G.N., Schultz, R.C., Isenhart, T.M., 2004. Stream bank erosion adjacent to riparian forest buffers, row-crop fields, and continuously-grazed pastures along Bear Creek in central Iowa. J. Soil Water Conserv. 59, 19–27.

Zhang, Y.K., Schilling, K.E., 2006. Increasing streamflow and baseflow in Mississippi River since the 1940s: effect of land use change. J. Hydrol. 324, 412–422. https://doi.org/10.1016/j.jhydrol.2005.09.033.